Piezoelectric and Magnetoelectric Properties of Lead Zirconate Titanate/Ni-Ferrite Particulate Composites

JUNGHO RYU,[1,2] ALFREDO VÁZQUEZ CARAZO,[1] KENJI UCHINO[1] & HYOUN-EE KIM[2]

[1]*International Center for Actuators and Transducers, Materials Research Laboratory, The Pennsylvania State University, University Park, PA 16802, USA*
[2]*School of Materials Science and Engineering, Seoul National University, Seoul, 151-742 Korea*

Abstract. Piezoelectric and magnetoelectric properties of magnetoelectric particulate composites with Lead Zirconate Titanate (PZT) and Ni-ferrite were investigated. The maximum magnetoelectric voltage coefficient, $(dE/dH)_{max}$, increased with higher sintering temperature up to 1250°C. Composites sintered at 1300°C, had dissolution of Fe ions into PZT, or interdiffusion between PZT and ferrite. Connectivity of the ferrite particles and sintering temperature were important factors for fabrication of this particulate composite. The composite added with 20 wt.% amount of Ni-ferrite, sintered at 1250°C for 2 hours, had the highest magnetoelectric voltage coefficient of 115 mV/cm · Oe at room temperature. This value is comparable to that of the $BaTiO_3$-$CoFe_2O_4$ based composites reported by Philips laboratory, and is 44% higher than other magnetoelectric particulate composites.

Keywords: magnetoelectric, composite, piezoelectric, magnetostrictive

1. Introduction

The magnetoelectric composites with piezoelectric and magnetostrictive material are of interest as transducers, which transform changes in a magnetic field into electric voltage and vice versa [1–3]. It can be used as a magnetic field sensor for an alternative tool of the Hall sensor for magnetic field measurement, or as an electric current measurement.

The first work on the magnetoelectric composites was done at the Philips Laboratory [3–7]. The magnetoelectric composites were prepared by unidirectional solidification of an eutectic composition of the quinary system Fe-Co-Ti-Ba-O (in situ composites) [4, 5]. The unidirectional solidification helps in the decomposition of the eutectic liquid composition into alternate layers of the constituent phase: a piezoelectric perovskite phase and a piezomagnetic spinel phase. Although the magnetoelectric voltage coefficient ($dE/dH = 130$ mV/cm · Oe) [5] was superior to single-phase materials such as Cr_2O_3, the unidirectional solidification process required high temperature, and a critical control over the composition especially when one of the components (oxygen) was gas, and the unexpected third phase appeared in the composites [6]. In 1978, they reported on sintered magnetoelectric composites of $BaTiO_3$ and $Ni(Co,Mn)Fe_2O_4$ with excess TiO_2 in terms of the particle size effect, the cooling rate, and the mole ratios of both the phases [6]. They reported a maximum value of the magnetoelectric voltage coefficient of 80 mV/cm · Oe in sintered magnetoelectric composites. However, this value was still lower than in situ composites, and it required special poling process for high magnetoelectric effect.

Sintered magnetoelectric composites have many advantages compared to in situ composites [6]. The sintered composites are much easier and cheaper in fabrication than in situ composites. Moreover, molar ratio of phases, grain size of each phase, and sintering temperature are easily controllable. These are some important issues in fabricating the sintered magnetoelectric particulate composites. First, no chemical reaction should occur between the piezoelectric and magnetostrictive materials during the sintering process. The chemical reaction may reduce

the piezoelectric or magnetostrictive properties of each phase. Second, the resistivity of magnetostrictive phase should be as high as possible. If the resistivity of magnetostrictive is low, the electric poling becomes very difficult due to leakage current. Also, the leakage current reduces the magnetoelectric properties of the composites. When the ferrite particles make connected chains, the electric resistivity of composites is reduced significantly, because of the low resistivity of ferrite. Therefore, good dispersion of the ferrite particles in the matrix is highly required in order to sustain sufficient electric resistivity of the composite. Third, mechanical defects such as pores in the interface between two phases should not exist in the composite for good mechanical coupling.

Lead Zirconate Titanate (PZT) is the most suitable piezoelectric material for the use in these composites because of their high piezoelectric properties. A magnetostrictive material with a high magnetostrictive performance should be chosen for the composites. Because magnetostrictive properties are present in most of magnetic materials, there are various choices of materials including the ferrites and the ferromagnetic metals. For particulate composites, resistivity of the magnetostrictive phase should be as high as possible, because the piezoelectric phase has resistivity of the order of 10^{12} Ohm·cm. Both the magnitude of the magnetostriction and the slope of the magnetostriction curve with respect to applied magnetic field should have a large value in order to achieve high values of pseudo-piezomagnetic coefficients in the magnetostrictive phase. In this regard, Ni-Ferrite doped with Co, Cu, Mn ($NiCo_{0.02}Cu_{0.02}Mn_{0.1}Fe_{1.8}O_4$) has been chosen for this particulate composite, because of their superior magnetostriction, magnetomechanical coupling factor, and electric resistivity [6, 8].

In this study, the amount of Ni-ferrite doped with Co, Cu, Mn particles was varied from 10 to 50 wt.%. The sintering temperature was also varied from 1100 to 1300°C to investigate the effect of the sintering temperature on the sintering behaviors, microstructures, piezoelectric, and magnetoelectric properties of these particulate composites. The microstructures of the composites, such as connectivity or distribution of Ni-ferrite particles and grain size of the PZT matrix, may be important for the resultant magnetoelectric properties. This study tried to clarify how to get the high magnetoelectric effect from particulate composites.

2.   Experimental Procedures

2.1.   Preparation of Particulate Composite

Reagent grade powders of NiO, Co_2O_3, CuO, MnO_2, Fe_2O_3 (Alfa Aesar Co., MA, USA) were used to prepare the Ni-Ferrite doped with Co, Cu, Mn ($NiCo_{0.02}Cu_{0.02}Mn_{0.1}Fe_{1.8}O_4$). The raw powder mixture was ball-milled using high purity 3Y-TZP (Tetragonal Zirconia Polycrystalline) ball media (Tosoh Co., Tokyo, Japan) in a polyethylene jar for 10 hours. The mixed slurry was dried and calcined for Ni-ferrite formation at 1000°C for 5 hours. After calcination, the calcined pieces were crushed and passed a stainless steel screen of #70 U.S. mesh and ball milled again to obtain fine particles. After ball milling, the particle size distribution was analyzed by laser counting method (Mastersizer S Ver. 2.15, Malvern Instruments Inc., MA, USA). The average particle size (d_{50}) was 3.23 μm. PZT (APC-840, American Piezoceramics Inc., PA, USA) and Ni-ferrite powders were mixed together by ball milling, with various ferrite contents from 10 to 50 wt.%, for 10 hours. Pellets of $\phi 15 \times 3$ mm were made in a hardened-steel die using a hydraulic press under a pressure of 30 MPa, and then isostatically pressed under a 272 MPa pressure in rubber bags with a wet cold-isostatic press. Pressureless sintering of the composites was performed in a silicon carbide resistance furnace with PZT atmosphere powder bed at 1100, 1150, 1200, 1250, and 1300°C for 2 hours. Sintered densities were measured by the Archimedes method. Some of the specimens were polished with 0.3 μm alumina polishing powders, and examined with a scanning electron microscopy (SEM, S-3500N, Hitachi Co., Tokyo, Japan) and X-Ray Diffractometer (XRD) for the polished surfaces. The average grain sizes were determined from the scanning electron micrographs by the linear intercept method with the conversion factor of 1.5 [9].

2.2.   Property Measurements

Gold was sputtered on the lapped surfaces for the electrode formation. The electroded specimens were poled in silicone oil at 60°C by applying a d.c. field of 3–1.5 kV/mm for 10 min. The piezoelectric and dielectric properties were measured using a piezo d_{33} tester and an impedance analyzer (HP4192A, Hewlett-Packard Co., USA).

The magnetoelectric property was measured in terms of the variation of the coefficient dE/dH as a function of d.c. magnetic bias field. An electromagnet (GMW 5403 Magnet, Power and Buckley Inc., New Zealand) was used for the bias field up to 0.25 T (2.5 kOe). The coefficient was measured directly as response of the sample to an a.c. magnetic input signal at 1 kHz and 1 Oe amplitude superimposed on the d.c. bias field, both parallel to the sample axis. A signal generator (33120A, Hewlett Packard Co., USA) was used to drive the Helmotz coils and generate the a.c. magnetic field. The voltage generated from the particulate composites was measured under an open circuit condition by using a differential amplifier based on the INA121 FET-input Instrumentation Amplifier from Burn-Brown Inc [10]. The output signal from the amplifier was measured with an oscilloscope (54645A, Hewlett Packard Co., USA). The output voltage divided by the thickness of the sample and the a.c. magnetic field gives the magnetoelectric voltage coefficient of the composites.

3. Results and Discussion

3.1. Sintering Behavior and Microstructures

Figure 1 is the X-Ray Diffraction (XRD) patterns for the particulate composite of 50 wt.% PZT—50 wt.% Ni-ferrite composition with different sintering temperatures. All the patterns were almost the same each other, and indicate no chemical reaction during sintering up to 1250°C. However, at 1300°C, the peak intensities of the ferrite phase were reduced remarkably. It might be caused by the dissolution of Fe ions in the ferrite into the PZT phase. This decreased the magnetostrictive properties of the ferrite and the efficiency of the mechanical coupling between the PZT and ferrite. There was no evidence of any other impurity and or the third phase in the sintered body.

The microstructure of the composite was studied by a Scanning Electron Microscope (SEM). The SEM micrographs of the particulate composites sintered at 1200°C for 2 hours are shown for various contents of the ferrite phase in Fig. 2. They showed two different phases distinctly; white regions, PZT and dark particles, ferrite. As indicated by XRD patterns, SEM microstructures of the composites did not show any third phase caused by chemical reaction or interdiffusion between two phases. However, there were some large pores, as compared with PZT and ferrite grain

sizes, and agglomeration of the ferrite particles with clusters of a few microns. Those could be found more frequently in the specimens containing 40 and 50 wt.% ferrite rather than 20 or 30% ferrite.

In this experiment, because we did not control the connectivity, the actual connectivity was 3–3 or a random mixture of islands of 3–0 and 0–3 connectivities [11]. This fact could exibit a great difference in piezoelectric and the magnetoelectric properties.

Figure 3 shows the microstructure of the samples containing 20% ferrite phases with various sintering temperatures. The particle size and distribution of Ni-ferrite were almost the same up to 1250°C. The average grain size of the matrix PZT phase was increased with increasing sintering temperature. Average grain sizes of the composites were 0.97, 1.22, and 1.86 μm for 1150, 1200, and 1250°C, respectively. However, the composites sintered at 1300°C showed very large pores and huge grains with dark spot. Uneven grain boundaries were also observed in Fig. 3(d). This uneven grain boundary seems to be a Diffusion Induced Grain Boundary migration (DIGM) [12]. In general, this DIGM structure is the evidence of the chemical composition gradients. Therefore, dissolution of Fe ions from ferrite into PZT can be expected in this composite, and it can be the reason of the deduction of sinterability, piezoelectric and magnetoelectric properties.

Sample density was measured by Archimedes liquid immersion method with Xylenes ($\rho = 0.861$ g/cm^3 at 20°C). All measurements for individual compositions were measured with more than 4 samples. Results on densification for various sintering temperatures are shown in Fig. 4. Densification was promoted with increasing sintering temperature and subsequently reached a maximum density at 1150°C for all compositions. At 1150°C, the sintered density was already sufficiently high for all composites and it decreased as the sintering temperature increased above 1250°C. This decrease in density seems to be mainly due to the dissolution or interdiffusion between PZT and ferrite phases as seen in the XRD patterns and SEM micrographs. In addition, large pores could be the reason of this density decrease. As compared with the surrounding matrix grain sizes as seen in the SEM micrographs, large pores could grow faster than shrinkage during sintering in the final stage [13]. This limitation of the densification due to large pores, found also in other systems [14], might have been formed by the stress caused by heterogeneities of sintering rate between PZT and ferrite.
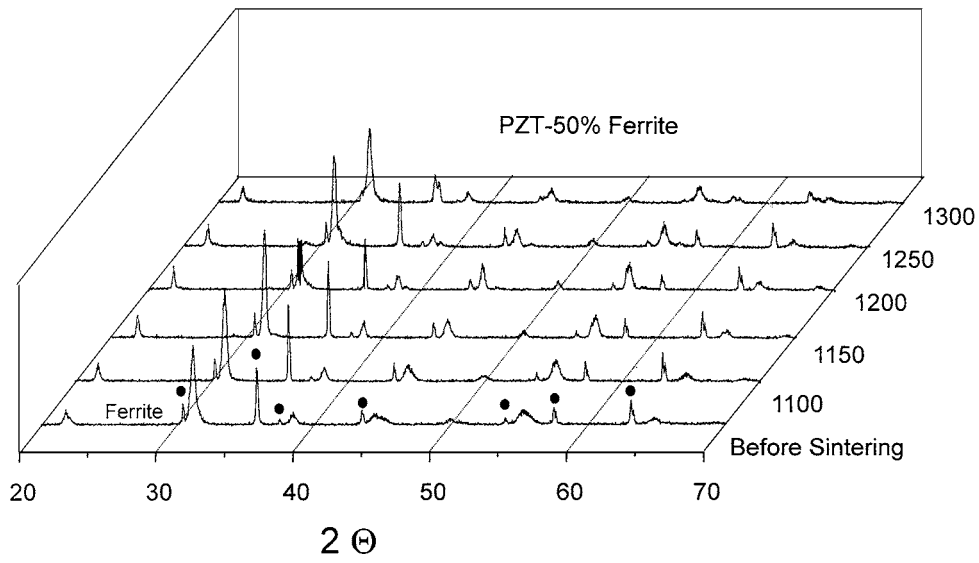
Fig. 1. X-Ray diffraction pattern of the composite with 50 wt.% Ni-ferrite particles as a function of sintering temperature.
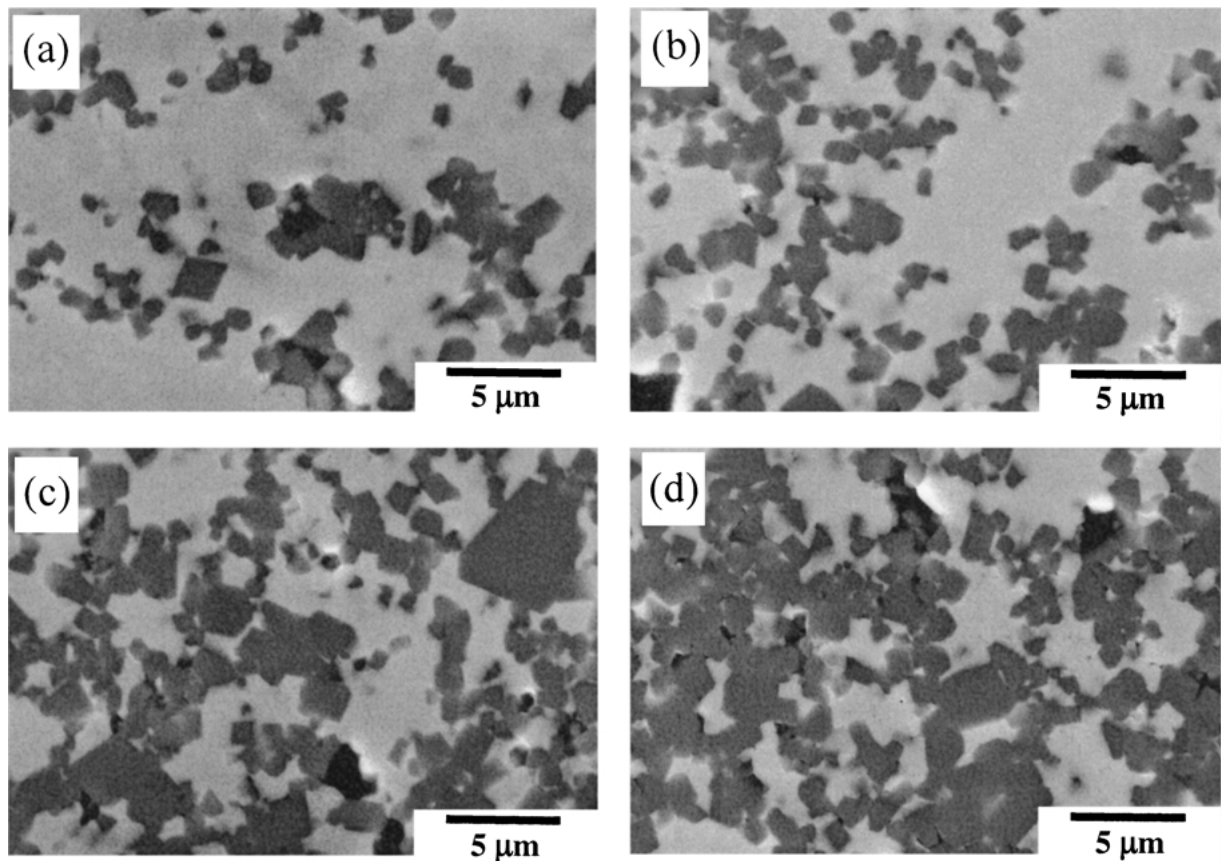

Fig. 2. SEM micrographs of the polished surfaces of the composites with (a) 20 wt.%, (b) 30 wt.%, (c) 40 wt.%, and (d) 50 wt.% Ni-ferrite particles, sintered at 1200°C for 2 hours.
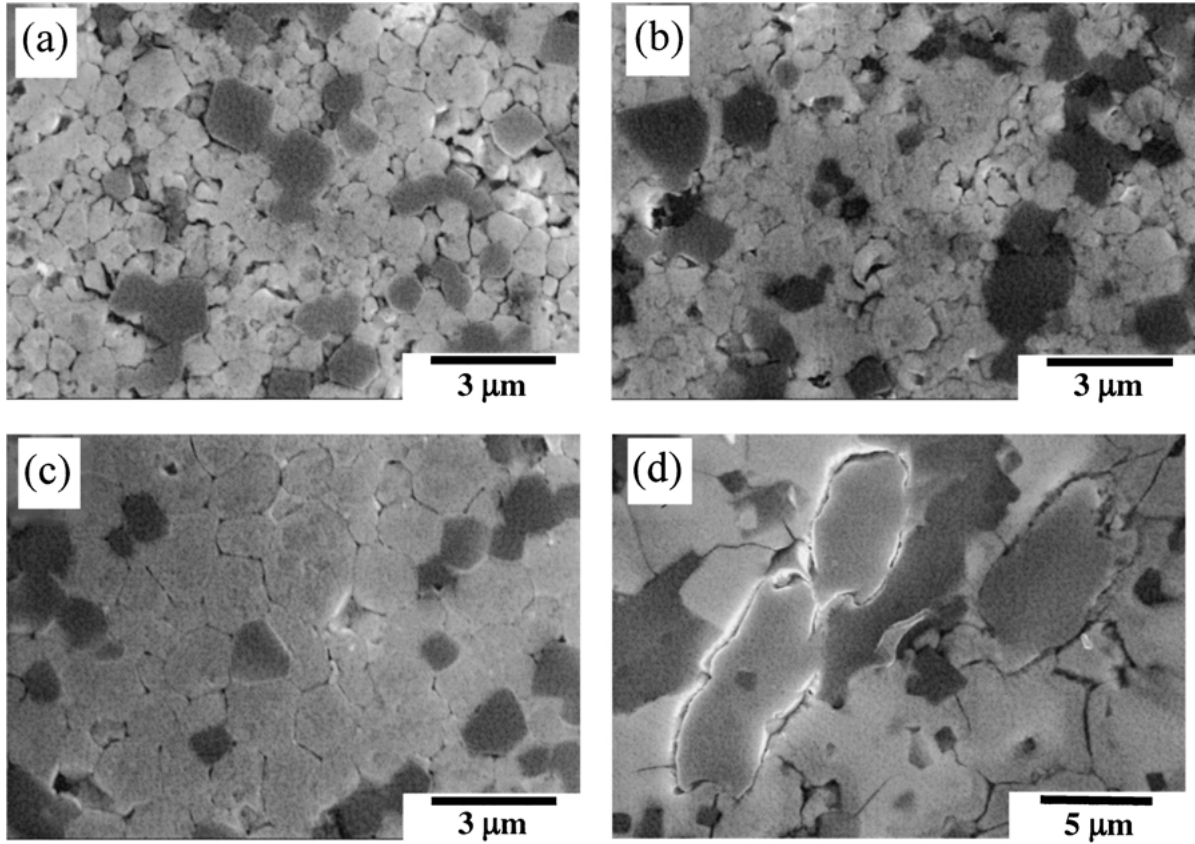
Fig. 3. SEM micrographs of the polished and chemically etched surfaces of the composite with 20 wt.% Ni-ferrite particles, sintered at (a) 1150°C, (b) 1200°C, (c) 1250°C, and (d) 1300°C for 2 hours.
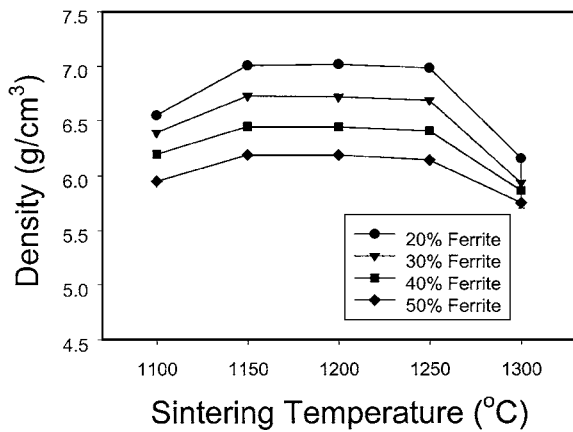

Fig. 4. Sintered density of the composites with a different amount of Ni-ferrite particles as a function of the sintering temperature.

3.2. Dielectric and Piezoelectric Properties

The composites had lower electric resistivity than pure PZT, and this was monitored in the dielectric measurements. Figures 5(a) and (b) show the dielectric constant and dielectric loss for these composites as a function of temperature. All specimens were sintered at 1200°C for 2 hours and electroded by gold sputtering. Samples containing smaller amount of ferrite particles showed the dielectric constant peak transition temperature close to the Curie temperature of pure PZT. However, as the content of ferrite increased, the transition peak shifted toward the lower temperature. With an increase of ferrite concentration, a jump was observed both in dielectric constant and loss curves. These jumps are merely due to the limitation of the measurement system for a low electric resistivity.
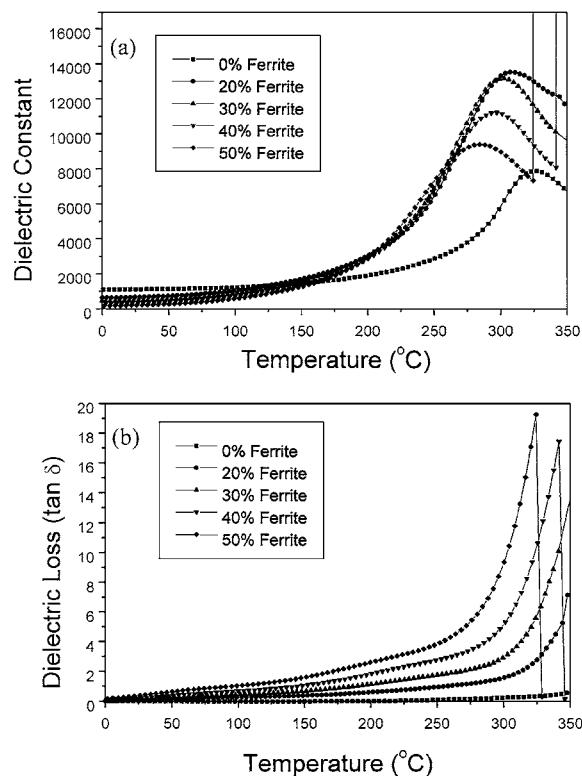
Fig. 5. Dielectric properties of the composites sintered at 1200°C for 2 hours as a function of temperature. (a) Dielectric constant and (b) Dielectric loss.

Fig. 6. Room temperature dielectric properties of the composites as a function of sintering temperature. (a) Dielectric constant and (b) dielectric loss.

The ferrite material has a small dielectric dipole, however, that is much smaller than the ferroelectrics material [15]. According to Deverin, a magnetic ordering might be responsible for dielectric changes with temperature [15]. Any change in the magnetic ordering should cause a dielectric change. In addition, the onset of the magnetic ordering may cause a change in electrical resistivity. It is reported that the increase in dielectric constant and dielectric loss corresponds to the increase of AC electric conductivity [16]. In this regard, the jump in the dielectric constant and dielectric loss at high temperature in Fig. 5 was caused by high AC electric conductivity of the ferrite phase at high temperature. As shown in the microstructures, the connectivity of ferrite particles increased with increasing ferrite content. Consequently, the composites with a higher amount of ferrite exhibited higher electric conductivity than others.

The room temperature dielectric constant and dielectric loss are plotted in Figs. 6(a) and (b), respec-
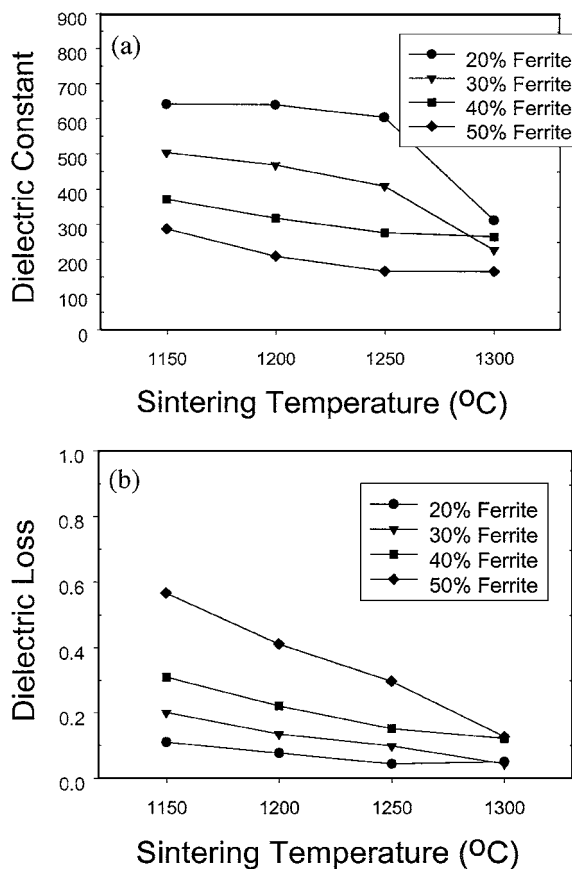
tively. The dielectric constant and dielectric loss of the composites decreased and increased with increasing ferrite content, respectively.

Figures 7(a) and (b) show the piezoelectric properties, d_{33} and g_{33}, for various compositions as a function of sintering temperature. The piezoelectric properties of the composites decreased with the amount of the ferrite phase, as similar to the dielectric properties. The piezoelectric properties changed slightly with sintering temperature. At 1200 or 1250°C, all compositions showed the best piezoelectric properties.

Figures 8, 9, and 10 show the magnetoelectric voltage coefficient as a function of the d.c. magnetic bias for 1150°C, 1200°C, and 1250°C sintered composites, respectively. The magnetoelectric voltage coefficient showed a maximum around 0.12 T for all composites except 10% ferrite particles added composites. The
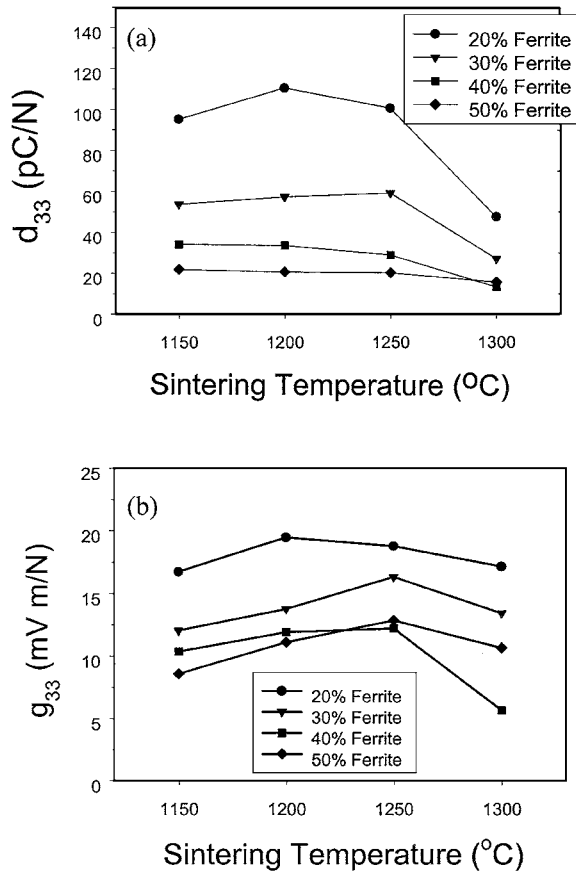
Fig. 7. Piezoelectric properties of the composites as a function of sintering temperature. (a) Piezoelectric constant d_{33} and (b) piezoelectric voltage constant g_{33}.
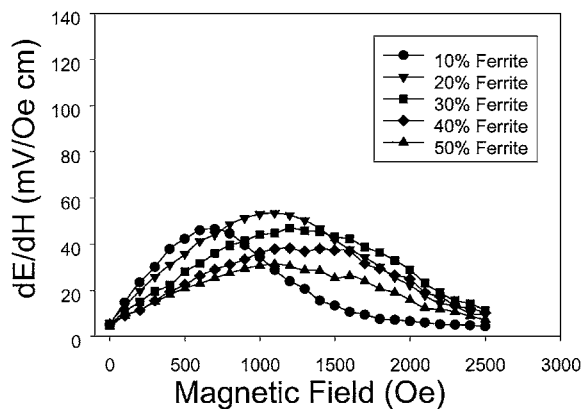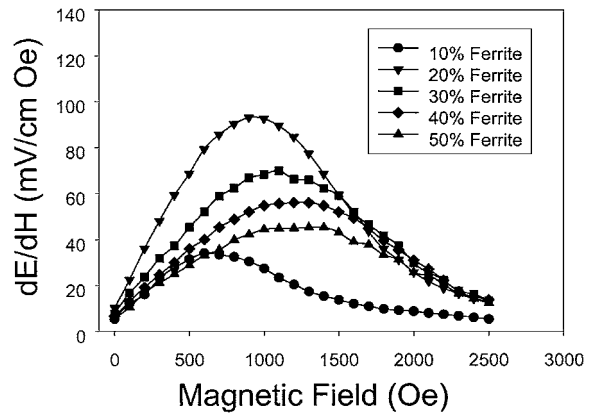

Fig. 9. Magnetoelectric voltage coefficient as a function of d.c magnetic bias field for the composites sintered at 1200°C for 2 hours.

Fig. 10. Magnetoelectric voltage coefficient as a function of d.c magnetic bias field for the composites sintered at 1250°C for 2 hours.
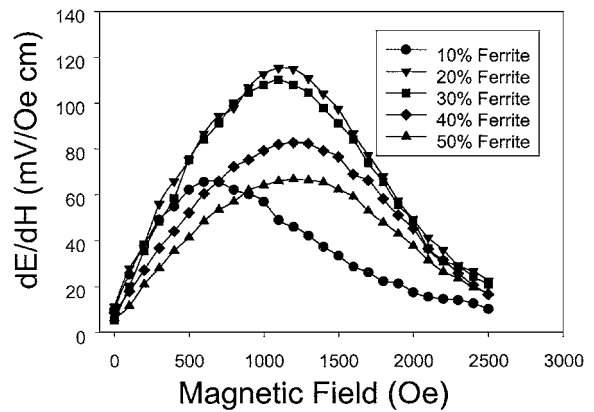

Fig. 8. Magnetoelectric voltage coefficient as a function of d.c magnetic bias field for the composites sintered at 1150°C for 2 hours.

composites with 20% ferrite particles added showed the higher magnetoelectric voltage coefficient for all sintering temperatures. As shown in the micrographs, the distribution of ferrite particles became more uniform and less connected when the amount of ferrite was low. Therefore, the highest magnetoelectric voltage coefficient with 20% ferrite particles in this study may be originated from more uniform distribution as well as less connection of ferrite particles i.e., higher electric resistivity. For the 10% ferrite added composite, the magnetoelectric voltage coefficient was not higher than that of the 20% ferrite added composite, due to too small amount of ferrite.

Figure 11 shows the maximum magnetoelectric voltage coefficient of each composite as a function
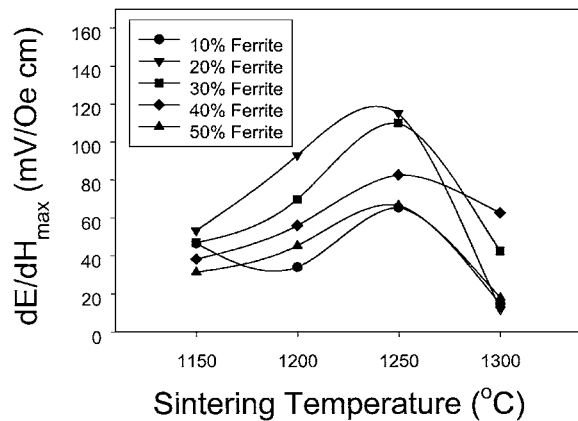
Fig. 11. Maximum magnetoelectric voltage coefficient of the composites as a function of sintering temperature.

of sintering temperature. When composites were sintered at 1250°C, the magnetoelectric voltage coefficient was maximum. It is known that the piezoelectric properties of PZT increase, when the grain size increases [17]. Thus, this seems to be caused by relatively large grain size of matrix PZT phase in the composites sintered at 1250°C as shown in the microstructure ($G_{av} = 1.86$ μm). A homogeneous and well dispersed microstructure and large grain size of the matrix PZT phase are the most important factors to get a high magnetoelectric voltage coefficient.

4. Conclusion

Magnetoelectric particulate composites were fabricated with PZT and Co, Cu, Mn doped Ni-ferrite ($NiCo_{0.02}Cu_{0.02}Mn_{0.1}Fe_{1.8}O_4$) by the conventional ceramic sintering process. Not only the connectivity of the ferrite phase, but also the sintering temperature are the important parameters for higher magnetoelectric

voltage coefficient (*dE/dH*). The chemical reaction of the PZT with ferrite, and connection of ferrite particles make it difficult to get high magnetoelectric effects. We obtained the highest magnetoelectric voltage coefficient from the composite of 20% ferrite added, sintered at 1250°C. The value was 115 mv/cm · Oe, which is 44% higher than previously reported value for the magnetoelectric particulate composite [6].

References

1. K. Uchino, in *Comprehensive Composite Materials: Piezoelectric Composites* (Elsevier, Amsterdam, The Netherlands, 2000), Vol. 5, chap. 5.24, p. 523.
2. T.H. O'Dell, *Electronics and Power*, **11**, 266 (1965).
3. J. Van Suchetelene, *Philips Research Report*, **27**, 28 (1972).
4. J. van den Boomgaard, D.R. Terrell, R.A.J. Born, and H.F.J.I. Giller, *J. Mater. Sci.*, **9**, 1705 (1974).
5. A.M.J.G. Van Run, D.R. Terrell, and J.H. Scholing, *J. Mater. Sci.*, **9**, 1710 (1974).
6. J. van den Boomgaard and R.A.J. Born, *J. Mater. Sci.*, **13**, 1538 (1978).
7. J. van den Boomgaard, A.M.J.G. Van Run, and J.Van Suchtelen, *Ferroelectrics*, **10**, 295 (1976).
8. T.G. Lupeiko, S.S. Lopatin, I.V. Lisnevskaya, and B.I. Zvyagintsev, *Inorg. Mater.*, **30**, 1353 (1994).
9. R.L. Fullman, *J. Metals Trans, AIME*, **197**, 447 (1953).
10. J. Ryu, A. Vázquez Carazo, K. Uchino, and H.E. Kim, *Jap. J. Appl. Phys.*, in print.
11. R.E. Newnham, *Ferroelectrics*, **68**, 1 (1986).
12. J.K. Park and D.Y. Kim, *J. Am. Ceram. Soc.*, **79**, 1405 (1996).
13. W.D. Kingery and B. Francois, in *Sintering and Related Phenomena: The Sintering of Crystalline Oxides, I. Interactions Between Grain Boundaries and Pores*, edited by G.C. Kuczynski, N. Hooten, and C. Gibson (Gordon & Breach Science Publishers, New York, 1967), p. 471.
14. J. Ryu and J. Lee, *The Korean Journal of Ceramics*, **3**, 199 (1997).
15. J.A. Deverin, *Ferroelectrics*, **19**, 9 (1978).
16. A. Fouskova and L.E. Cross, *J. Appl. Phys.*, **41**, 2834 (1970).
17. C.A. Randall, N. Kim, J.-P. Kucera, W. Cao, and T.R. Shrout, *J. Am. Ceram. Soc.*, **81**, 677 (1998).